Lasers in Manufacturing Conference 2019

Influence of laser spot size, exposure time and power on the mechanical & topological properties of Ti-6Al-4V lattice structures

Darragh S. Egan[a*], Denis P. Dowling[a]

[a]*I-Form Advanced Manufacturing Research Centrer,Dublin, Dublin, Ireland*

Abstract

Selective Laser Melting facilitates the fabrication of complex cellular structures, exhibiting high strength to weight ratios. In this study Ti-6Al-4V lattice structures were fabricated using a 500 W, pulsed, Yb:YAG laser. The effect of laser power (50 to 150 W), exposure time (350 to 750 µs) and laser spot size (75 to 106 µm ø) on the structures mechanical and topological properties was evaluated. The energy input level of the laser directly influences the size of the melt pool, which in turn determines the diameter of the struts, not the CAD file, within these structures. As a result, structures with relative porosity in the range of 83.8 to 96.6 % were obtained. The laser power was found to have the most significant impact on compression strength, which increased by 96 % as laser power was increased from 50 to 150 W.

Keywords: Additive Manufacturing, Selective Laser Melting Metals, Lattice structures, Laser energy;

Introduction

Additive manufacturing (AM) is a process where parts are fabricated layer by layer [1]. This process allows for the creation of complex structures that cannot be fabricated using traditional methods [2]. The development of AM is largely driven by the medical, automotive and aerospace industries, this is due to the advantageous properties that they possess. [3][4][5].

Selective laser melting (SLM) is an AM technique that can easily produce complex shaped metallic parts, such as cellular structures [6]. Lattice structures are a type of cellular structure that are composed of a non-stochastic in-fill structure, and a high volume of open pores. These type of structures are of interest due to the high strength to weight ratios they can achieve [7][8]. To fabricate lattice structures using the SLM

* Corresponding author. Tel.: +353-87-6631376
E-mail address: darragh.egan@i-form.ie

technique, some researchers have used a “single-exposure” method [9]. In this method, instead of the laser scanning a contour and hatching a cross sectional area, it fires a single exposure at a defined point for a defined period of time. This results in the strut diameter being equal to the width and shape of the melt-pool. Therefor, as the process parameters dictate the size of these individual meltpools, it is vitally important to understand the effect that they have in order to achieve desirable strut diameters.

To the authors knowledge, there have been no reports published which have;

(a) assess the effect of increasing the laser beam spot size on the properties of cellular structures,

(b) assess the effect of varying the laser power, exposure time and laser beam spot size on both the strut and major pore size diameter, within diamond based non-stochastic cellular structures,

(c) compares the effect that adjusting the theoretical energy input through either laser power, exposure time or laser spot size variations has on the structures mechanical properties.

1. Material and methods

1.1. Materials & manufacturing

In this study a Renishaw RenAM500M SLM machine was used to produce lattice structures, using the single exposure method. This scale system is fitted with a 500 W Yb:YAG (λ = 1.07 µm) laser, with gaussian beam profile, with an in-focused laser beam diameter of approximately 75 µm ($1/e^2$). The RenAM500M is a “modulated” system, in that the laser fires for a given amount of time after which it switches off and moves a defined distance to the next point location before firing again for a given time. To increase the laser spot size, the focal offset distance (FOD) was varied. Increasing the FOD value from 0, results in the focal plane of the laser been shifted below the build plate. This in turn results in the laser spot size on the build plate increasing.

1.2. Test specimen

All samples were fabricated using Ti-6Al-4V Extra Low Interstitials-0406 grade 23 powder, with typical powder particle diameters in the range 15 to 45 µm, obtained from AP & C. Samples were built to the ISO 13314 requirements, which explains the method of compression testing porous metallic structures. The samples had dimension of 15x15x28 mm (L x W x H), as shown in Figure 1. This figure also illustrates the 1.5 mm diamond unit cell used to in this work. This cell type was chosen due to its potential application in the biomedical industry, due to its close packing, along with the ease at which it can be produced using SLM methods. After the build process, the samples were removed from the build plate and cut to a length of 20 mm using a precision saw, following which they were washed in an ultrasonic bath and dried.

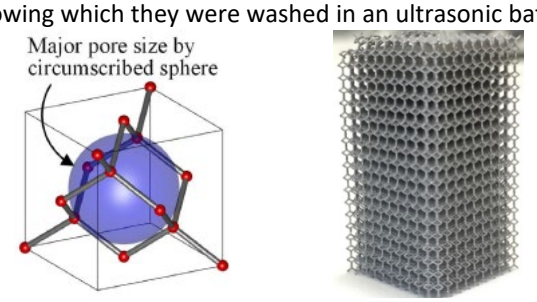

Fig. 1. Schematic showing diamond unit cell and the major pore size within the cell (left). Example of a printed Ti6Al4V lattice structure (right).

To analyse the effect of laser power (*P*), exposure time (*t*) and laser spot size on the structural properties, samples were built by varying the laser power and exposure time, between 50 and 150 W and 350 to 750 µs respectively, independently of each other, resulting in 25 variations. To assess the effect of increasing the laser spot size on the lattice structure's properties, parts were printed at five different FOD values, i.e. laser spot sizes. The FOD values were set to 0.0, 1.8 2.5 3.1 and 3.6 mm, with the maximum FOD value been equal to the Rayleigh length of the beam, all at constant power and exposure time.

To compare the effects of the different process parameters used, the total energy input (*E'*) was used as a metric, and was calculated using equation 1, adopted from [10] and [11],

$$E' = \frac{Pt}{\pi\omega^2 l} \quad \left[{}^{\mu J}/_{\mu m^3}\right] \qquad \text{Equ.1}$$

where, P is the laser power, t is the exposure time, *l* is the layer height and ω is the beam radius. ω is a function of the FOD and can be theoretically calculated using equation 2 [10],

$$\omega(z) = \omega_0 \sqrt{1 + \left(\frac{z}{z_r}\right)^2} \ [\mu m] \qquad \text{Equ.2}$$

where z, ω_0 and z_r is the FOD, the in-focused beam waist and the Rayleigh length of the beam respectively.

1.3. Quasi-static testing

Static compression testing, according to ISO 13314, was used to determine the mechanical properties of the structures [12]. Testing was carried out using a Tinius Olsen 50 kN machine, using either a 10 or 50 kN load cell, depending on the lattice type being tested, at a strain rate of ~10^{-2} strain/second. A minimum of four samples of each structure variation was tested.

1.4. Characterisation

Detailed images of the structures was obtained via Scanning Electron microscopy, on a Hitachi EM4000Plus, this also facilitated the measurement of the strut diameters. The diameter of the major pores within the lattice structures was calculated using equation 3 below,

$$\emptyset_{pore} = \emptyset_{pore}^{max} - \emptyset_{strut} \qquad \text{Equ.3}$$

where, $\emptyset_{pore}$ is the pore diameter, $\emptyset_{strut}$ is the respective strut diameter and $\emptyset_{pore}^{max}$ is the theoretical maximum pore size at an infinitesimally small strut diameter, and was determined using the Rhino CAD software.

The dry weighing method was used to obtain the relative density, $\bar{\rho}$, of each structure. Using this method, the mass of each structure was divided by the theoretical mass of the macro-volume. Where the density of bulk Ti-6Al-4V was taken to be 4.42 g/cm^3. A Mettler Toledo balance was used to measure the weight of each specimen to within 10 µg. The relative porosity, $\bar{\Phi}$, of each structure was calculated using equation 4, adopted from [13].

$$\bar{\Phi} = 1 - \bar{\rho} \qquad \text{Equ.4}$$

2. Results & discussion

The effect of increasing the FOD, and thus the laser beam spot size, on the structures relative porosity, strut diameter and major pore diameter can be seen in Figure 2. It is observed, that as the laser spot size is increased the structures relative porosity increases by just 1.5 % from 89 to 90.5 %, while the strut

diameters within the structures decrease by 17 %, from 235.3 to 195.3 µm. This change can be attributed to the decrease in input energy associated with increasing the laser spot size. Correspondingly, by increasing the FOD the intensity at the center portion of the beam decreases, due to the change in beam profile associated with the de-focusing of the laser. This results in less material been melted by the laser, and therefore less material been bonded together, during each firing of the laser. This in turn results in smaller strut diameters been created and an increase in relative porosity been obtained.

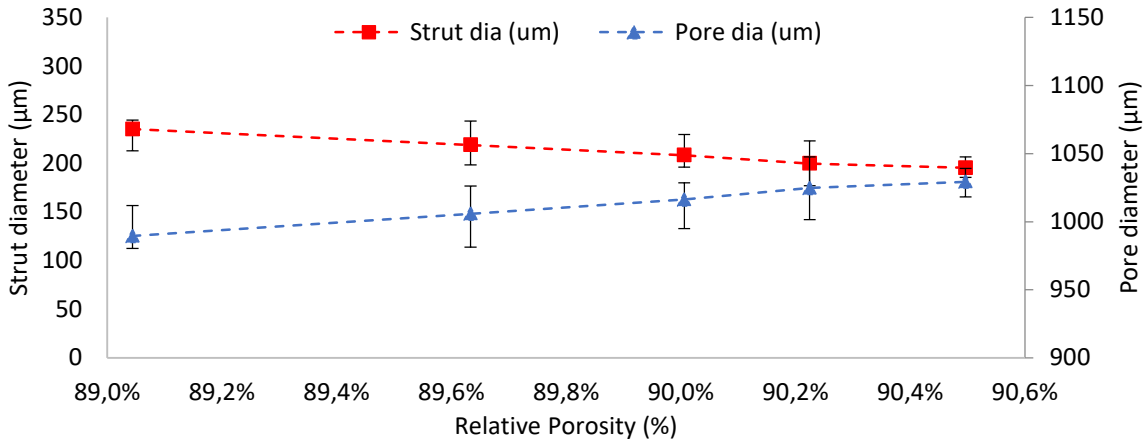

Fig. 2. Effect of relative porosity when plotted against strut diameter and pore diameter.

Figure 2 also shows the relationship between the structure's relative porosity, the strut diameter and the pore diameter. This result effectively shows that as the structures relative porosity increases, due to a reduction in the individual strut diameters from 235.3 to 195.3 µm, the pore diameter increases from 989.5 to 1029.4 µm. This is due to the greater amount of free space within each unit cell, caused by the reduced strut diameters.

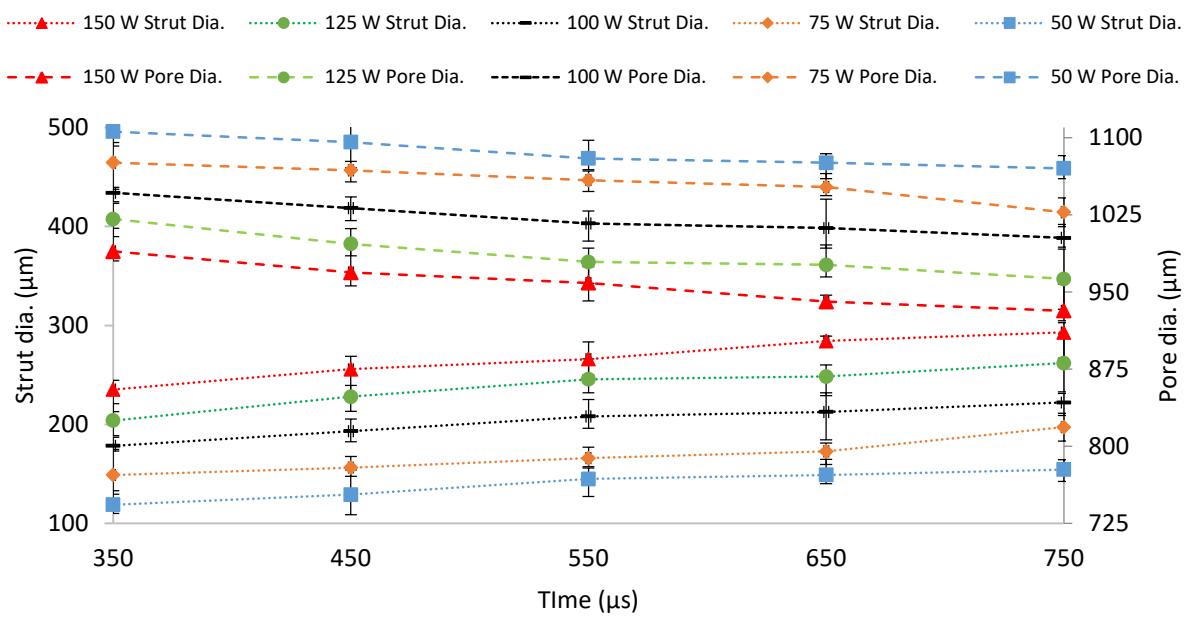

Fig. 3. Effect of exposure time at different laser powers on the structures strut and major pore diameters.

The effect of increasing the laser power and exposure time on the relative porosity of the lattice structures and on the strut and major pore diameters within the structures, is shown in Figure 3 and Figure 4. By increasing the laser power from 50 to 150 W, at a constant exposure time of 350 µs, the strut diameter in the respective structures increased from 118.9 to 154.6 µm, while the relative porosity of the structures decreased from 96.3 % to 89.1 %. At the highest exposure time used of 750 µs, increasing the laser power from 50 to 150 W resulted in the structures strut diameters increasing from 235.3 to 292.9 µm, while the relative porosity of the structures decreased from 94 % to 83.8 %. A similar trend occurs for all the other power and time variations, as shown in Figure 4.

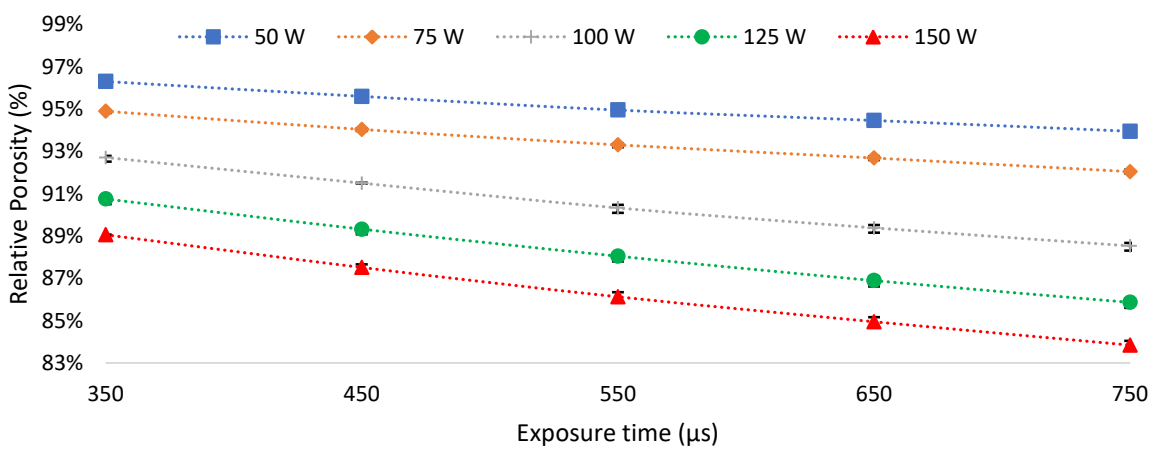

Fig. 4. Effect of exposure time at the different laser powers shown on the relative porosity of the lattice structures.

As demonstrated in Figure 4, with increasing laser exposure time from 350 to 750 µs, for each of the power variations, a near linear decrease in the lattice structure relative porosity occurs. The increased line slopes associated with the higher laser power levels, 100 to 150 W, shows that the effect of increasing the exposure time on the structures relative porosity has a greater effect at higher laser power levels, than at lower powers. This occurs due to the higher cumulative energy input associated with higher laser power at longer exposure times, compared to the energy input at lower powers at similar exposure times. The increase in strut diameter and respective decrease in relative porosity and major pore diameter, as the energy input is increased, occurs due to the following reason. As the laser input energy is increased, more material is melted, resulting in larger meltpools, this in turn solidifies and results in the increased strut diameter.

The strength (σ) and Youngs modules (E) of the structures increased with the relative density of the structure, or in this case decrease with increasing relative porosity, as described by Gibson and Ashby [14].

$$\frac{\sigma}{\sigma_0} = C_1 \left(\frac{\rho}{\rho_0}\right)^n \quad \text{Equ.3}$$

$$\frac{E}{E_0} = C_2 \left(\frac{\rho}{\rho_0}\right)^m \quad \text{Equ.4}$$

Where σ_0 and E_0 are the strength and Young's modulus of the solid base material, and C, n and m are constants. The structures created with an energy input of 0.85 ($\mu J/\mu m^3$), at 150 W and 750 µs, achieved a first maximum compressive strength (CS) of 44.7 MPa. In contrast the structures created with an energy input of 0.13 ($\mu J/\mu m^3$), at 50 W and 350 µs, achieved a CS of 0.278 MPa.

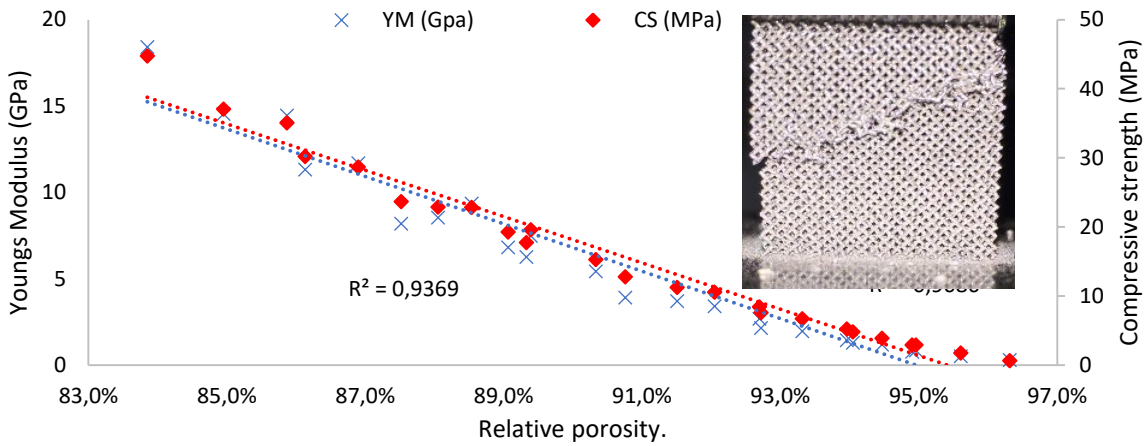

Fig. 5. Effect of increasing the input energy input on the Youngs modulus and compressive strength of the lattice structures. Insert: Lattice structure undergoing fracture during compression testing.

The trends illustrated in Figure 5 are as anticipated, in that as the relative porosity of the structures increase, due to an decreasing strut diameter, the compressive strength and Youngs modulus of the structures also decrease. The results seen here are promising from a biomedical point of view, in that the Youngs modulus and compressive strength achieved are in the typical range of that of human trabecular and cortical bone, which have values of 0.1-4.5 to 3-20 GPa and from 2-17 to 33-193 MPa respectively [15][16].

3. Conclusions

In this study the effect of varying the three key SLM laser process parameters on the properties of Ti-6Al-

4V diamond based cellular structures has been investigated together. The following conclusions and findings can be drawn from the results obtained in this study;

a) The effect of laser beam spot size was investigated on these types of structures. It was demonstrated that through a 100 % increase in the laser spot size, the strut diameter within the structures reduced by 17 %, while the relative porosity of the structures increased by just 1.6 %.

b) 25 variations of power and exposure time were investigated (50 < W < 150 and 350< µs> 750). It has been shown that as the laser power and/or the exposure time increase the relative porosity of the structures decreases. It was demonstrated that as the strut diameter within the 1.5 mm unit cells increased from 119 to 193 µm, due to the increasing energy input, the major pore diameter within the structures decreased from 1,106 to 932 µm.

c) While increasing the laser beam spot size has a significant effect on the theoretical energy input, its impact on the structures properties was not found to be as significant as the effect of reducing laser power or exposure time. At constant energy input levels, lattice structures created using a focused laser exhibited up to 23% smaller strut diameters than structures created using a de-focused laser. Thus, demonstrating that the mode of energy input is critical to achieving the desired part properties.

Acknowledgement

This work was supported by the SFI funded I-Form Advanced Manufacturing Research Centre (16/RC/3872). The authors would also like to thank Renishaw PLC and Croom Precision Medical for their technical advice.

References

[1] T. Vilaro, C. Colin, J.D. Bartout, As-fabricated and heat-treated microstructures of the Ti-6Al-4V alloy processed by selective laser melting, Metall. Mater. Trans. A Phys. Metall. Mater. Sci. 42 (2011) 3190–3199. doi:10.1007/s11661-011-0731-y.

[2]. A. Slotwinski, E.J. Garboczi, P.E. Stutzman, C.F. Ferraris, S.S. Watson, M.A. Peltz, Characterization of Metal Powders Used for:Additive Manufacturing, J. Res. Natl. Inst. Stand. Technol. Charact. 119 (2014) 25–29.

[3] D. Herzog, V. Seyda, E. Wycisk, C. Emmelmann, Additive manufacturing of metals, Acta Mater. 117 (2016) 371–392. doi:10.1016/j.actamat.2016.07.019.

[4] M. Javaid, A. Haleem, Additive manufacturing applications in medical cases : A literature based review, Alexandria J. Med. 54 (2018).

[5] O. Santoliquido, G. Bianchi, P. Dimopoulos Eggenschwiler, A. Ortona, Additive manufacturing of periodic ceramic substrates for automotive catalyst supports, Int. J. Appl. Ceram. Technol. 14 (2017) 1164–1173. doi:10.1111/ijac.12745.

[6] C. Yan, L. Hao, A. Hussein, D. Raymont, Evaluations of cellular lattice structures manufactured using selective laser melting, Int. J. Mach. Tools Manuf. 62 (2012) 32–38. doi:10.1016/j.ijmachtools.2012.06.002.

[7] L. Xiao, W. Song, Additively-manufactured functionally graded Ti-6Al-4V lattice structures with high strength under static and dynamic loading: Experiments, Int. J. Impact Eng. 111 (2018) 255–272. doi:10.1016/j.ijimpeng.2017.09.018.

[8] D.S.J. Al-Saedi, S.H. Masood, M. Faizan-Ur-Rab, A. Alomarah, P. Ponnusamy, Mechanical properties and energy absorption capability of functionally graded F2BCC lattice fabricated by SLM, Mater. Des. 144 (2018) 32–44. doi:10.1016/j.matdes.2018.01.059.

[9] L. Mullen, R.C. Stamp, W.K. Brooks, E. Jones, C.J. Sutcliffe, Selective laser melting: A regular unit cell approach for the manufacture of porous, titanium, bone in-growth constructs, suitable for orthopedic applications, J. Biomed. Mater. Res. - Part B Appl.

Biomater. 89 (2009) 325–334. doi:10.1002/jbm.b.31219.

[10] T.D. McLouth, G.E. Bean, D.B. Witkin, S.D. Sitzman, P.M. Adams, D.N. Patel, W. Park, J.M. Yang, R.J. Zaldivar, The effect of laser focus shift on microstructural variation of Inconel 718 produced by selective laser melting, Mater. Des. 149 (2018) 205–213. doi:10.1016/j.matdes.2018.04.019.

[11] W.A. Ayoola, W.J. Suder, S.W. Williams, Parameters controlling weld bead profile in conduction laser welding, J. Mater. Process. Technol. 249 (2017) 522–530. doi:10.1016/j.jmatprotec.2017.06.026.

[12] I. Standard, ISO 13314 Mechanical testing of metals, ductility testing, compression test for porous and cellular metals, Ref. Number ISO. 13314 (2011) 1–7. doi:ISO 13314:2011.

[13] B. Van Hooreweder, Y. Apers, K. Lietaert, J. Kruth, Improving the fatigue performance of porous metallic biomaterials produced by Selective Laser Melting, Acta Biomater. 47 (2017) 193–202.

[14] M.F. Ashby, The properties of foams and lattices, Philos. Trans. R. Soc. A Math. Phys. Eng. Sci. 364 (2006) 15–30. doi:10.1098/rsta.2005.1678.

[15] E.F. Morgan, T.M. Keaveny, Dependence of yield strain of human trabecular bone on anatomic site, J. Biomech. 34 (2001) 569–577.

[16] F. Linde, I. Hvid, The effect of constraint on the mechanical behaviour of trabecular bone specimens, J. Biomech. 22 (1989).